Environ. Eng. Res. Vol. 12, No. 3, pp. 109~117, 2007
Korean Society of Environmental Engineers

CHARACTERISTICS OF RESIDUAL CARBON DERIVED FROM THE COMBUSTION OF VACUUM RESIDUE IN A TEST FURNACE

Ho Young Park*, and Sang Il Seo

Power Generation Laboratory, Korea Electric Power Research Institute,
103-16 Munji-Dong, Yusung-Gu, Daejon 305-380, South Korea
(received , accepted)

Abstract : The characteristics of carbonaceous particles collected from the combustion of Vacuum Residue (VR) in a test furnace have been investigated. The physical and chemical characterization includes particle size, scanning electron microscopy of the surface structure, measurement of porosity, surface area and density, EDX/XRD analyses and measurement of chemical composition. The studies show that the carbonaceous VR particles are very porous and spheroidal, and have many blow-holes on the surface. The particles become smaller and more sponge-like as the reaction proceeds. The present porosity of VR particles is similar to that of cenospheres from the combustion of heavy oil, and the majority of pores are distributed in macro-pores above 0.03 μm in diameter. Measurements of pore distribution and surface area showed that the macro-pores contributed most to total pore volume, whereas the micro-pores contributed to total surface area.

Key Words : Density, Porosity, SEM, Surface area, Vacuum residue

INTRODUCTION

Vacuum Residue (VR) is defined as the fraction of petroleum that does not evaporate under vacuum in the distillation process. It has an atmospheric equivalent boiling point over 525ºC and is produced as the bottom product from the vacuum distillation column in a refinery. VR has been usually used to manufacture asphalts for road pavement.[1)]

Recently, there have been vigorous efforts in Japan to use it as a fuel for direct combustion in utility boiler.[2-6)] MHI (Mitsubishi Heavy Industries) provided 25 boilers fired by asphalt or high-viscosity heavy oils and a 475 ton/hr steam based boiler fired by VR, which began commercial operation in July 1998.[5)] The operation results of a 274 MW power plant, which is burning VR, were also reported by Aoki et al. (2004).[6)]

As compared with heavy oil, VR has many difficulties to be utilized in utility boiler due to its extremely high viscosity and high percentages of sulphur, nitrogen, carbon residue and heavy metals. Among several problems associated with the utilization of VR as a fuel for combustion and gasification, a great care should be exerted on the reaction of carbonaceous particles, and it has been addressed in elsewhere.[2,4,6,7)]

In heavy oil combustion, there have been many studies on the physical and chemical characteristics of carbonaceous particles.[8-14)] However, studies on the carbonaceous VR particles were rarely found. Ichinose et al. (1998)[2)] reported

* Corresponding author
E-mail: hypark@kepri.re.kr
Tel: +82-42-865-5498, Fax: +82-42-865-7573

that the major problem in VR firing is the high percentage of unburned carbon and the poor reactivity of VR carbon char compared with that of bituminous coal char.

Prior to the present study, the VR combustion tests were performed with the small-scale test furnace (fuel feeding rate of 20kg/h, 0.2m in inner diameter and 2.5m in length).[15] The carbonaceous VR particles were collected along the furnace axis and at the exhaust. The lack of any prior physical characterization of this VR residual particle led us to investigate its properties.

The focus of this study is on the physical and chemical characterization of carbonaceous VR particles collected from the test furnace. The characterization includes particle size, scanning electron microscopy of the surface structure, porosity, surface area, density, EDX and XRD analysis as well as chemical composition.

EXPERIMENTAL

Preparation of Samples

Samples of carbonaceous residue were taken from the VR combustion test at Korea Electric Power Research Institute (KEPRI) in South Korea. The test furnace, as seen in Figure 1, was cylindrical, down-fired and operated in atmospheric pressure. The inner diameter and height of the furnace are 200 mm and 3200mm, respectively. The furnace wall is refractory and thermal insulation to minimize the heat loss, and the respective radial thickness are 200 and 147 mm. The VR burner is installed on the top of the furnace, so that the flame develops along the furnace axis. The burner used has an inner diameter of 105 mm with a steam atomized, internal mixing type nozzle. The VR was supplied from Hyundai Oil Bank refinery. The composition of VR is C: 85.30%, H: 10.34%, O: 0.13%, N: 0.45% and S: 3.78% (weight basis). Combustion tests were performed at various equivalence ratios. Among several tests, the present VR carbonaceous samples were obtained from fuel rich flame (equivalence ratio of 1.525).

The samples used in this study were collected

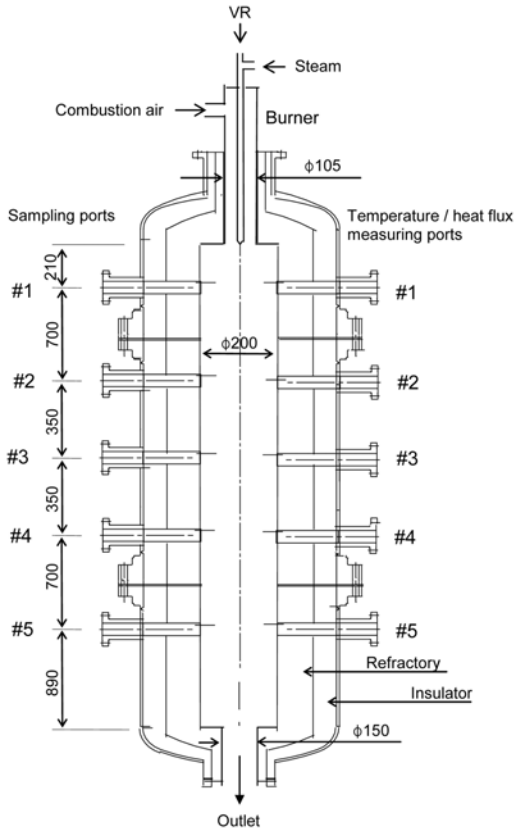

Figure 1. Schematic diagram of a test furnace.

at the first sampling port and at the exhaust, and they were designated as sample I and II, respectively. The detailed information on the VR combustion test and sampling method can be found in Park and Kim (2006).[15]

Particle Analysis

The changes in particle diameter were examined by the laser scattering technique (Helos system supplied by Sympatec Gmbh). The surface structure of solid samples was studied using a JEOL JSM 6360 scanning electron microscope (SEM). EDX and XRD analyses were also carried out with INCA X-sight (Oxford Instruments) and D/MAX-2200 (Rigaku international Co.).

For characterizing particle structure, ASAP 2405 (Micromeritics) was employed to determine N_2 surface area of solid sample. Mercury porosimeter (Autopore III 9420, Micromeritics) was used to obtain mercury densities and pore distri-

butions. Helium density was determined by helium displacement at room temperature. An Accupyc 1330 (Micromeritics) was used.

RESULTS AND DISCUSSION

VR Combustion Test

Figure 2 shows the measured axial gas temperature, O_2, CO and CO_2 concentrations along the furnace. The measured particle diameters are also given. The respective feed rates of VR and combustion air were 14.21 kg/hr and 97.5 Nm^3/hr, which correspond to the equivalence ratio of 1.525. The atomizing steam fed into the nozzle was 4.68 kg/hr. The gas analyzer, IMR 3000 (Environmental Equipment Inc.), was used to measure concentrations of O_2, CO, CO_2, NO and SO_2 at five sampling ports. The distribution of axial gas temperature was measured with a 0.125 mm B-type thermocouple at five temperature measuring ports. At the first port, the temperature measurement was not available since the fast injection of atomized VR droplets caused failure of the ceramic-shielded thermocouple.

Although the gas temperature at port No. 1 could not be measured, the initial gas temperature rise up to the second port (x=910mm) would be steeper than the temperature decline downstream. For major species concentrations, the oxygen decreases rapidly from the burner to the axial position of 910 mm while CO_2 is formed rapidly in this region. After the first 910 mm of the furnace, oxygen is depleted to zero and CO_2 shows flat profile. Considering O_2 and CO_2 profiles together with the profiles of temperature and particle size, the main reaction zone seems to be formed within 910 mm from the burner tip. The CO increases to the first 910 mm of the furnace and the profile is flattened. The gas analyzer used in the present work, IMR 3000 (Environmental Equipment Inc.), was not possible to measure CO and CO_2 concentrations exceeding 6000 ppm and 15.9 %, respectively. Concentrations of CO and CO_2 measured downstream in Figure 2 exceeded these ranges, so that only the upper limit values have to be presented. It is expected that the downstream flame is in fuel rich environment and the actual values would be clearly higher than the measured ones. Overall, Figure 2 shows the typical profiles of a fuel-rich flame, and a recognizable amount of carbonaceous VR particles were collected at exhaust. Comments on the particle size will be presented in the next section.

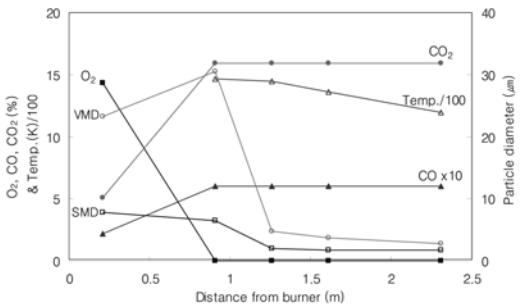

Figure 2. Distributions of gas concentration, temperature and particle diameter along with the furnace.

Particle Size and Morphology

The sauter mean diameters (SMD) of VR particles collected at axial positions of 210, 910, 1260, 1610 and 2310 mm were 7.80, 6.47, 2.02, 1.75 and 1.73 μm, respectively. The corresponding volume mean diameters (VMD) were 23.17, 30.55, 4.72, 3.67 and 2.78 μm (See Figure 2). The diameter decreases abruptly from the relatively higher value at x=910 mm to lower value at x=1260 mm, suggesting that the particle reaction mainly occurs before x=1260mm. The continuous, slight decrease in particle diameter is observed downstream. The available oxygen for the oxidation of carbon residue is depleted downstream, resulting in no further decrease in particle diameter. In this work, the formation of carbonaceous particle seems to be accomplished within the first 210 mm from the burner (See Figure 1).

The SEM photograph of sample I is given in Figure 3(a), and it tells us the particles are spheroidal and have many blow-holes. Some broken particles seem to be layered and flaky. The EDX analysis did not be carried out for sample I. Other sample collected at port No. 1, as given in Figure 3(b), shows that tiny particles are found in everywhere and cover a large particle.

These tiny particles are thought to be soot particles. The co-existence of carbon char and soot particles was also identified in the VR combustion test performed by Ichinose et al. (1998).[2] The result of EDX analysis on the surface of particle, as seen in Figure 3(b), gave values of 81.06% C, 12.12% O, 5.12% S, 0.12% V, 0.90% Cu and 0.67% Zn (weight basis).

The magnification of tiny particles is given in Figure 3(c). It is noticed that an individual par-

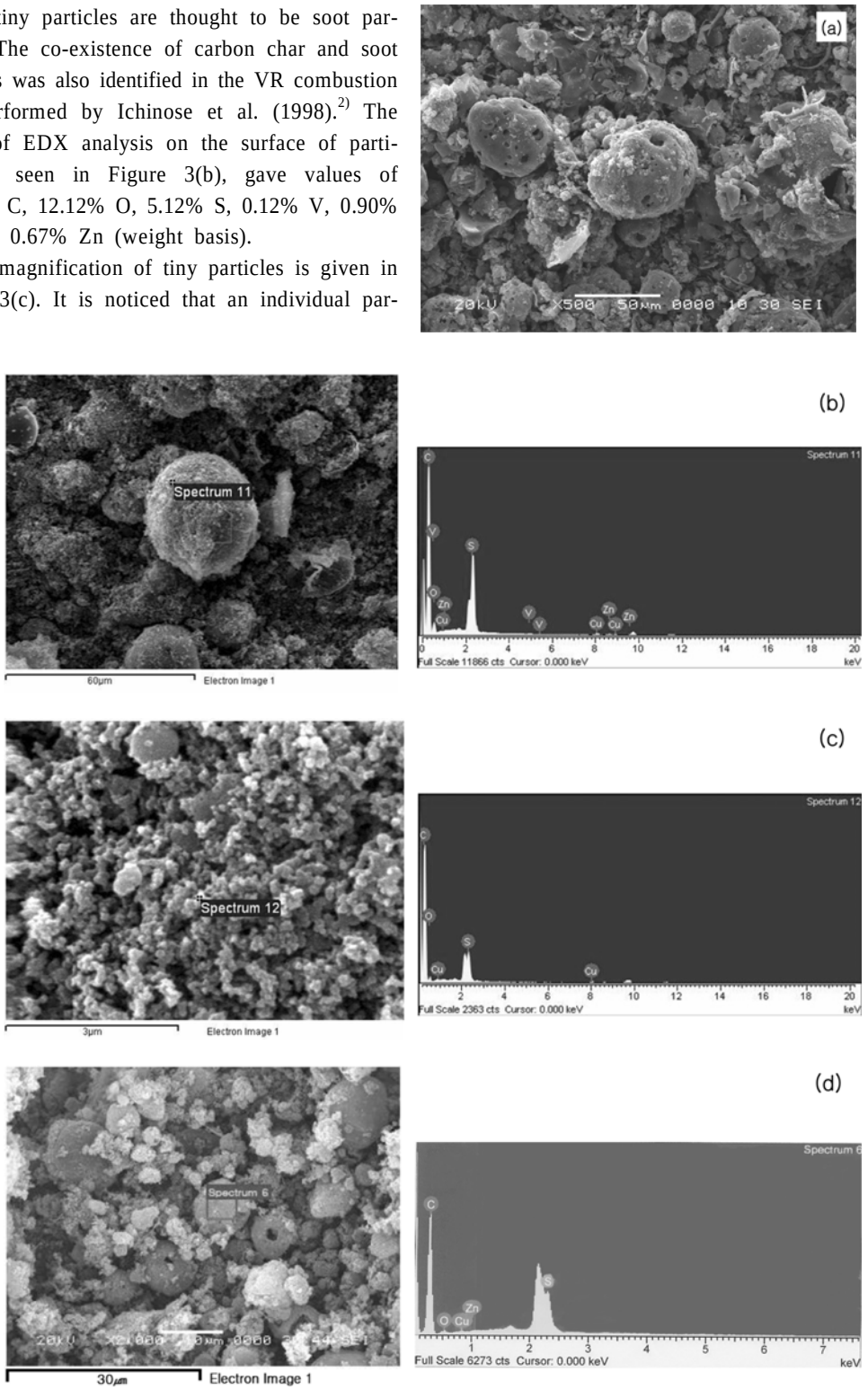

Figure 3. SEM photographs of particles collected at (a) port No. 1, (b) port No. 1 (soot), (c) port No. 1 (magnification of soot), (d) the exhaust.

ticle diameter is about 100 nm. The EDX analysis on the surface of tiny particle gave values of 85.61% C, 9.77% O, 2.96% S and 1.66% Cu (weight basis). Both EDX analyses in Figure 3 (b) and (c) revealed that substantial amounts of sulphur are still remained in the particles, and the higher percentage of carbon was found in soot particle. Here, the Cu is detected in EDX analysis as not found in the parent VR elemental analysis. It might come from the contamination of the sample during the sampling procedure since the present sampling system used the bronze sintered filter as well as the cyclone.

Sample II, collected at the exhaust, is shown in Figure 3(d). The particles are smaller and more sponge-like than those in sample I. Some particles are hollow and have voids within the shell. EDX analysis gave values of 84.37% C, 5.29% O, 2.75% S, 4.15 Cu and 3.44 Zn% (weight basis).

Chemical Composition and Crystal Structure

Elemental analyses were carried out for sample I and II. The obtained values of C, H, N, S and unidentified materials for sample I were 68,17, 3.40, 1.29, 5.16 and 21.97 wt.%, respectively. For sample II, the corresponding values were 43.54, 1.45, 1.55, 10.35 and 43.11 wt.%. The oxygen was not included in the elemental analysis. It is difficult to make an acceptable interpretation with these values. However, the findings of nitrogen and sulphur in samples suggest that some of these elements are not fully devolatilized from the atomized VR droplets and still remained in the solid particles, especially in fuel-rich condition.

The crystal structure of carbon contained in the samples (see Figure 4) was analyzed by the X-ray diffractometry (XRD). Crystallite height, L_c, and diameter, L_a, were obtained from the (002) and (10) diffraction peaks, respectively. For sample I and II, the XRD pattern gave the (002) and (10) carbon peaks at about 24 and 44°, respectively. Graphitic interlayer spacing, d_{002}, was also obtained. Table 1 summarizes the crystallite size for sample I and II. There is no

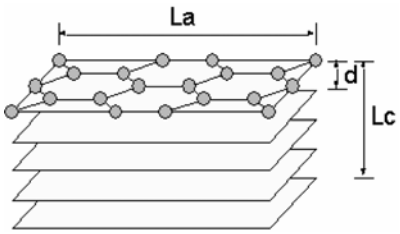

Figure 4. Crystal structure of carbon.

Table 1. Crystallite dimensions of sample I and II

	L_c (Å)	L_a (Å)	d_{002} (Å)
Sample I	7	12	3.715
Sample II	9	27	3.612

distinct difference in d_{002} and L_c. The sample II is thought to be much more reacted particle than sample I since the sample II was collected at the exhaust. Regardless of the extent of particle reaction, the present VR carbonaceous particle gives the unchanged graphitic interlayer spacing, d_{002}, and crystallite height, L_c. This finding was also reported in the gasification study of coal char.[16] With respect to the crystallite diameter, L_a, sample II gives somewhat higher value compared with sample I. Generally, increase in crystallite diameter (L_a) with the unchanged crystallite height (L_c) means decrease in the ratio of edge (active) carbon atoms to basal (inactive) carbon atoms.[17] Although the present XRD gives some different values in L_a for both samples, it is difficult to draw a meaning interpretation since clear distinction between basal and edge sites is very difficult with small crystallite size in this study, that is, $L_a = 12 \sim 27$Å.

Density, Porosity and Surface Area

The investigation of pore structure of carbonaceous VR particles was carried out for the sample I and II, and the results are summarized in Table 2. In this study, pore structure has been investigated in the diameter range 0.0046 - 2.34 μm, and pores have been divided into macro-pores (0.03 - 2.34 μm), transitional pores (0.0046 - 0.03 μm), and micro-pores (below 0.0046 μm). The apparent density of the particles, ρ_a (g/mL), was measured with mercury intrusion at 94 psi

Table 2. Physical properties of carbonaceous VR particles

	ρ_a (g/mL)	ρ_{tr} (g/mL)	ρ_{mi} (g/mL)	ρ_{He} (g/mL)	ε_T	ε_{ma}	ε_{tr}	ε_{mi}	V_T (mL/g)	V_{ma} (mL/g)	V_{tr} (mL/g)	V_{mi} (mL/g)	S_{Hg} (m^2/g)	S_{BET} (m^2/g)
Sample I (port no. 1)	0.421	0.934	1.147	2.252	0.813	0.549	0.084	0.180	1.929	1.302	0.199	0.428	78.0	38.7
Sample II (exhaust)	0.484	1.164	1.277	2.105	0.77	0.584	0.037	0.149	1.590	1.207	0.076	0.308	54.5	43.4

assuming that the inter-particle voids and intra-particle voids with openings larger than 2.34 μm are excluded in the intrusion volume. With regard to the pressure at which inter and intra-particle voids are filled, this pressure has been experimentally determined with the mercury penetrated volume curve versus the pore diameter.[18] Here, there might be some uncertainty in obtaining the apparent density since the blow holes up to 10μm in diameter, easily visible in Figure 3(a), are presented on the particle surface.

Mercury densities, ρ_{tr} and ρ_{mi} (g/mL), corresponding to the solid plus pores below 0.03 and 0.0046 μm in diameter, were measured at 7171 and 49906 psi, respectively. The total porosity, ε_T, was calculated from the apparent density, ρ_a (g/mL), and the helium density, ρ_{He} (g/mL). The porosities corresponding to macro, transitional and micro-pores (ε_{ma}, ε_{tr} and ε_{mi}) were calculated from the above density values. These are calculated with the following equations:

$$\varepsilon_T = \left(1 - \frac{\rho_a}{\rho_{He}}\right) \times 100 \tag{1}$$

$$\varepsilon_{ma} = \left(1 - \frac{\rho_{tr}}{\rho_a}\right) \times 100 \tag{2}$$

$$\varepsilon_{tr} = \rho_a \left(\frac{1}{\rho_{tr}} - \frac{1}{\rho_{mi}}\right) \times 100 \tag{3}$$

$$\varepsilon_{mi} = \rho_a \left(\frac{1}{\rho_{mi}} - \frac{1}{\rho_{He}}\right) \times 100 \tag{4}$$

The specific total pore volume, V_T (mL/g), and the specific pore volumes for macro, transitional and micro-pores (V_{ma}, V_{tr} and V_{mi}) could be determined by the combination of helium, apparent and mercury densities. These are calculated with the following equations:

$$V_T = \frac{1}{\rho_a} - \frac{1}{\rho_{He}} \tag{5}$$

$$V_{ma} = \frac{1}{\rho_a} - \frac{1}{\rho_{tr}} \tag{6}$$

$$V_{tr} = \frac{1}{\rho_{tr}} - \frac{1}{\rho_{mi}} \tag{7}$$

$$V_{mi} = \frac{1}{\rho_{mi}} - \frac{1}{\rho_{He}} \tag{8}$$

Table 2 indicates that VR particles sampled are very porous, and the majority of pores are distributed in macro-pores above 0.03 μm in diameter. These observations are consistent with the hollow, porous structure established microscopically. The present total porosities, ε_T, having a value of 0.81 and 0.77 are very compatible with the porosity of cenospheres, which is 0.82, from the combustion of heavy oil.[8] For sample I and II, the respective portions of micro-pore volume to the total pore volume are about 22 and 19%. The portions of transitional pores, which are about 10 and 6% respectively, are relatively small.

The pore area penetrated by mercury, S_{Hg}, is also given in Table 2, together with N_2 BET surface area, S_{BET}. The N_2 surface area and pore size distribution were determined using the BET equation. On the while, the pore area from porosimetry, S_{Hg}, is calculated assuming cylindrical pores. The value of S_{Hg} for sample I is higher than that for sample II, whereas the values of S_{BET} give the higher surface area in sample II that in sample I. Agreement between SHg and SBET is so poor. It might come from the fact that the measured pore range (0.0042 - 2.34 μm) in porosity measurement is also differed with

the range (0.0012 - 0.112 μm) in N_2 BET measurement.

For sample II, the distributions of pore volume and area based on the mercury intrusion porosimetry are given in Figure 5(a) and (b). The pore sizes are mainly distributed at 0.03 - 2.0 μm, which shows that most are macro-pores. The contribution to the surface area is prominent with the smaller pores below 0.2 μm in diameter, as seen in Figure 3(b). Figure 5(c) and (d) show the pore distributions determined by N_2 adsorption measurement, and represent the smaller pores below 0.01 μm in diameter contribute most to the surface area, on the while very little to the pore volume.

Figure 6(a) and (b) show the pore volume and area distribution for sample I. Macro-pores accounts for most of the volume, while contributing very little to the pore area. There is distinct peak around 0.03 μm in pore volume distribution, resulting in sharp increase in pore area distribution. As seen in Figure 6(c) and (d), N_2 BET adsorption shows that pores below 0.01 μm is responsible for most area, and have little contribution to the volume. Comparing with Figure 5(a) to (d), the total pore volume and area of sample I are bigger than those of sample II. Overall, the macro-pores contribute most to total pore volume, whereas micro-pores contribute most to total surface area.

CONCLUSIONS

Carbonaceous VR particles obtained from the combustion of vacuum residue in a test furnace were investigated. Under the fuel-rich combustion environments, atomized VR droplets do not be fully oxidized, and consequently the flame produce recognizable amounts of unburned carbon particles. Carbonaceous VR particles are very porous and spheroidal, and have many blow-holes on the surface. Tiny particles, thought to be soot, were also found near the burner nozzle.

For the VR particles collected at port No. 1 and the exhaust, the respective total porosities of 0.81 and 0.77 are very compatible with the

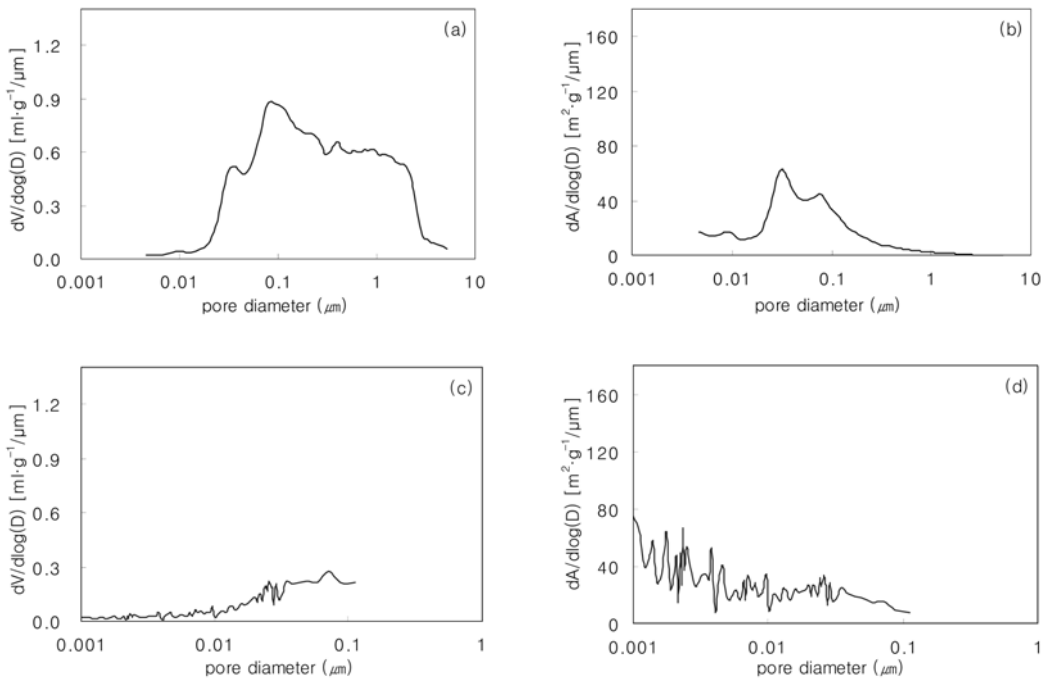

Figure 5. Pore distributions of particles for sample II ; (a) pore volume by porosimetry, (b) pore area by porosimetry, (c) pore volume by N_2 adsorption, (d) pore area by N_2 adsorption.

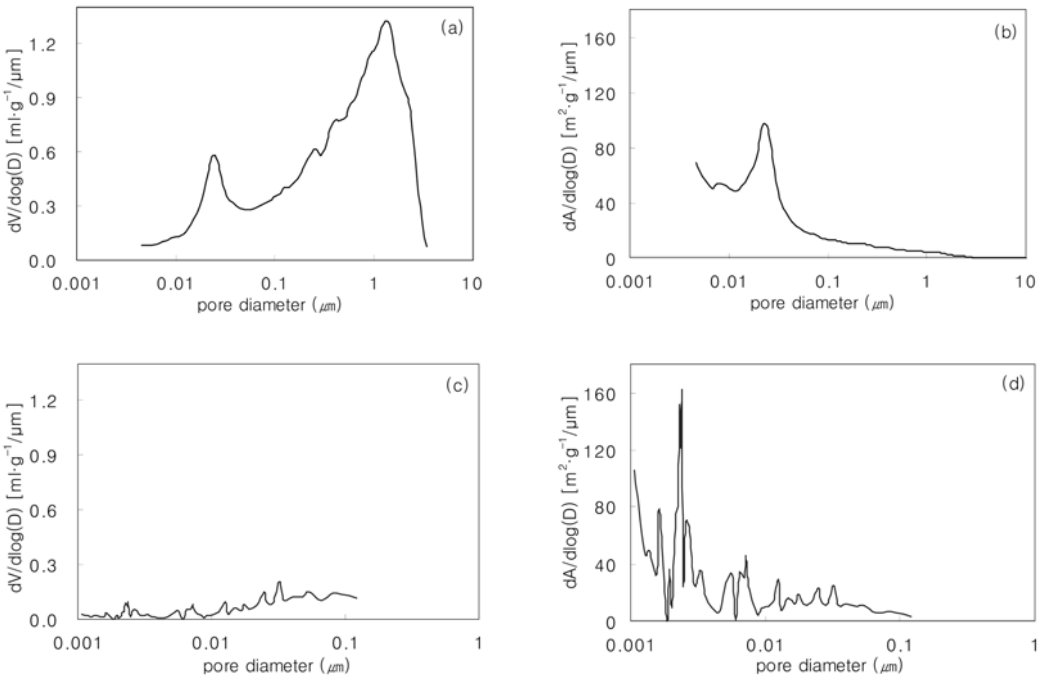

Figure 6. Pore distributions of particles for sample I ; (a) pore volume by porosimetry, (b) pore area by porosimetry, (c) pore volume by N_2 adsorption, (d) pore area by N_2 adsorption.

reported porosity of cenospheres from the combustion of heavy oil. Both samples have a small percentage of transitional pore volume but higher level of macro pore volume. The porosity, pore volume and area of the particles collected at port No. 1 give the higher values than those at the exhaust. Measurements of pore distribution and surface area by mercury porosimetry and N_2 BET adsorption technique show that the macro-pores contribute most to total pore volume, whereas the micro-pores contribute most to total surface area.

REFERENCES

1. Gray, M. R., Upgrading petroleum residues and heavy oils, Marcel Dekker, New York, pp. 1-6 (1994).
2. Ichinose, T., Fujimura, K., Takeno, K., Motai, T., Arakawa, Y., and Fujii, H., "Combustion characteristics and pollution minimum technology for VR (Vacuum Residue) fired boiler," *JSME International Journal*, **41**, 1055-1060 (1998).
3. Minoru, H., "Demonstrative operation plan of asphalt burning power plant in oil refinery," in *17th WEC congress*, Huston, USA (1998).
4. Hashimoto, A., Ichinose, T., Fujimura, K., Kaneko, S., Hishida, M., and Arakawa, Y., "Development of low excess air combustion technology for residual oil fuels," *Mitsubishi Juco Giho*, **35** (1998). See also http://www.mhi.co.jp/tech/htm/8351/e835108a.htm.
5. Fujimura, K., Mastumoto, H., Arakawa, Y., Fujii, H., and Mizoguchi, T., "Development and operation results of VR firing boiler," *Mitsubishi Juco Giho*, **36** (1999). See also http://www. mhi.co.jp/tech/htm/9362/e936211a.htm.
6. Aoki, H., Fukushima, H., and Yoshida, T., "Design and operation results of vacuum residue firing boiler (Japanese)," *The thermal and nuclear power*, **55**, 1356-1362 (2004).
7. Park, H. Y., and Kim, T. H., "Non-isothermal pyrolysis of vacuum residue (VR) in a thermogravimetric analyzer," *Energy Conversion and Management*, **47**, 2118-2127 (2006).

8. Clayton, R. M., and Back, L. H., "Physical and chemical characteristics of cenospheres from the combustion of heavy fuel oil," *Journal of Engineering for Gas Turbines and Power*, **111**, 679-84 (1989).
9. Northrop, P. S., Gavalas, G. R., and Levendis, Y. A., "Combustion characteristics of carbonaceous residues from heavy oil fired boilers," *Energy & Fuels*, **5**, 587-94 (1991).
10. Seggiani, M., Vitolo, S., and Narducci, P., "Investigation on the porosity development by CO_2 activation in heavy oil fly ashes," *Fuel*, **82**, 1441-1450 (2003).
11. Hsieh, Y. M., and Tsai, M. S., "Physical and chemical analyses of unburned carbon from oil-fired fly ash," *Carbon*, **41**, 2317-2324 (2003).
12. Allouis, C., Beretta, F., and D'Alessio, A., Structure of inorganic and carbonaceous particles emitted from heavy oil combustion," *Chemosphere*, **51**, 1091-1096 (2003).
13. Caramuscio, P., Stefano, L. D., Seggiani, M., Vitolo, S., and Narducci, P., "Preparation of activated carbons from heavy-oil ashes," *Waste Management*, **23**, 345-351 (2003).
14. Bertran, C. A., and Marques, C. S. T., "Study of the particulate matter emitted from residual oil combustion and natural gas reburning," *J. Braz. Chem. Soc*., **15**, 548-555 (2004).
15. Park, H. Y., and Kim, Y. J., "Combustion characteristics of vacuum residue in a test furnace and its utilization for utility boiler," *Korean J. of Chem. Eng.*, **24**(1), 83-92 (2006).
16. Kajitani, S., Hara, S., and Matsuda, H., "Gasification rate analysis of coal char with a pressurized drop tube furnace," *Fuel*, **81**, 539-546 (2002).
17. Radovic, L. R., Walker, P. L., and Jenkins, F. G., "Importance of carbon active sites in the gasification of coal chars," *Fuel*, **62**, 849-856 (1983).
18. Gan, H., Nandi, S. P., and Walker, P. L., "Nature of the porosity in American coals," *Fuel*, **51**, 272-277 (1972).